# Sequestering of the Prehairpin Intermediate of gp41 by Peptide N36$^{Mut(e,g)}$ Potentiates the Human Immunodeficiency Virus Type 1 Neutralizing Activity of Monoclonal Antibodies Directed against the N-Terminal Helical Repeat of gp41[▽]

Elena Gustchina,[1] Carole A Bewley,[2] and G. Marius Clore[1]*

*Laboratories of Chemical Physics*[1] *and Bioorganic Chemistry,*[2] *National Institute of Diabetes and Digestive and Kidney Diseases, National Institutes of Health, Bethesda, Maryland 20892-0520*

Human immunodeficiency virus type 1 (HIV-1) neutralization can be effected by several classes of inhibitors that target distinct regions of gp41 that are accessible in the prehairpin intermediate (PHI) state and block the formation of the six-helix bundle (6-HB) conformation of gp41. The N-heptad repeat (N-HR) of gp41 is the site of action of two classes of inhibitors. One class binds to the trimeric N-HR coiled coil, while the other, exemplified by the peptide N36$^{Mut(e,g)}$, disrupts the trimer and sequesters the PHI through the formation of heterotrimers. We recently reported a neutralizing Fab (Fab 3674), selected from a nonimmune phage library, that binds to the trimeric N-HR coiled coil through an epitope that remains exposed in the 6-HB and is also present in heterotrimers of the N-HR and N36$^{Mut(e,g)}$ peptide. Here we show that N36$^{Mut(e,g)}$ prolongs the temporal window during which the virus is susceptible to neutralization by the bivalent Fab 3674 and that bivalent Fab 3674 and N36$^{Mut(e,g)}$ neutralize HXB2 and SF162 strains of HIV-1, as well as isolates of diverse primary B and C HIV-1 strains, synergistically in a Env-pseudotyped virus neutralization assay. N36$^{Mut(e,g)}$ also rescues neutralizing activity of Fab 3674 against resistant virus strains and renders a series of related nonneutralizing Fabs neutralizing. Moreover, N36$^{Mut(e,g)}$ exhibits the same effects on the broadly neutralizing 2F5 and 4E10 monoclonal antibodies directed against the membrane-proximal extended region of gp41. The mechanistic implications of these findings are discussed.

Human immunodeficiency virus type 1 (HIV-1) infection is initiated by fusion of the virus with the target cell membrane (1, 11, 19, 40, 43, 51). The initial event involves the binding of the envelope (Env) protein gp120 first to CD4 and subsequently to the chemokine receptor, thereby triggering a series of conformational changes that lead to the formation of a prehairpin intermediate (PHI) of the second Env protein, gp41. In the PHI (14) gp41 bridges the viral and target cell membranes (Fig. 1). The PHI is tethered to the viral membrane by a transmembrane domain that lies C terminal to the C-heptad repeat (C-HR) (residues 623 to 663) and to the target membrane by the N-terminal fusion peptide. The exposed N-heptad repeat (N-HR) (residues 542 to 591), which lies C terminal to the fusion peptide, forms a parallel helical coiled-coil trimer. Apposition of the viral and target cell membranes is driven by the formation of a six-helix bundle (6-HB) conformation of gp41 comprising a trimer of hairpins in which the N-HR trimeric coiled coil is surrounded by three C-HR helices. The 6-HB represents the only structure of gp41 that has been solved to date by either crystallography (5, 49, 52) or nuclear magnetic resonance (3). The PHI is the target of four

classes of fusion inhibitors (4, 11, 26, 43). Class 1, 2, and 4 inhibitors simply bind to the N-HR, C-HR, and membrane-proximal extended region (MPER) of the PHI, respectively, thereby blocking the formation of the 6-HB (Fig. 1). Examples of class 1 inhibitors include peptides derived from the C-HR sequence (e.g., T20/enfuvirtide, C34, and membrane-anchored C-HR peptides) (20, 28, 31, 33, 53), cyclic D-peptides derived by mirror image phage display of the N-HR trimer (13), and several designed neutralizing antibodies (Abs) (e.g., D5, Fab 3674, and 8K8) (17, 29, 34, 37); class 2 inhibitors comprise various engineered constructs that present an exposed, stable N-HR trimeric coiled coil (e.g., N$_{CCG}$-gp41, N35$_{CCG}$-N13, 5-helix, and IQ-N23) (12, 25, 27, 44); and class 4 inhibitors comprise neutralizing monoclonal Abs (MAbs) derived from patients (e.g., 2F5 and 4E10) (36, 41, 47, 55). There is only a single example of a class 3 inhibitor, namely, the N36$^{Mut(e,g)}$ peptide (2), in which all the residues at helical positions *e* and *g* of the N-HR sequence have been mutated such that N36$^{Mut(e,g)}$ forms a monodisperse trimer that can no longer interact with the C-HR (Fig. 2A). N36$^{Mut(e,g)}$, like the class 1 inhibitors, targets the N-HR, but its mode of action is quite distinct from those of all three other classes of inhibitors (2, 16); specifically, N36$^{Mut(e,g)}$ inhibits trimerization of the N-HR by sequestering the N-HR into heterotrimers (Fig. 1).

Although the N-HR is highly conserved, its accessibility during the course of fusion is limited both sterically and temporally (15, 18, 46). The latter probably accounts for the dearth of naturally occurring neutralizing Abs targeting the N-HR, while
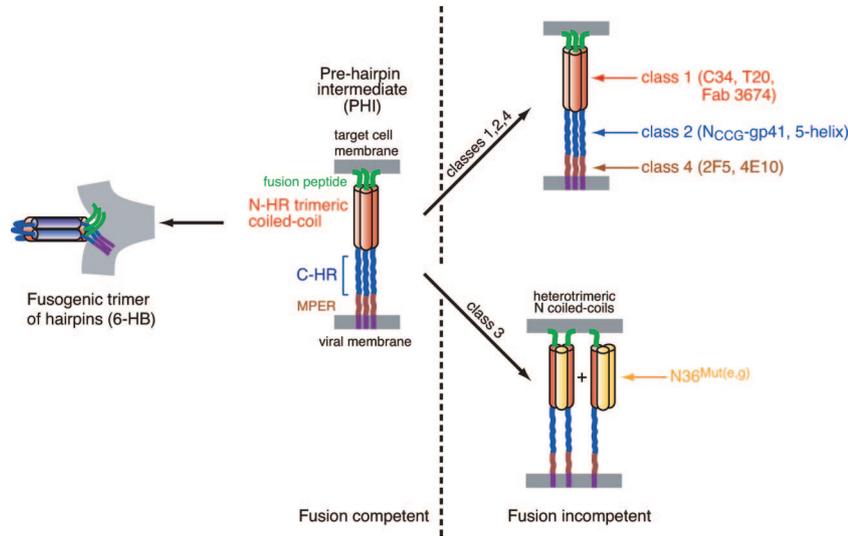
FIG. 1. Schematic of the sites of action of the four classes of inhibitors that target the PHI state of gp41. Class 1 inhibitors bind to the N-HR, class 2 inhibitors bind to the C-HR, class 3 inhibitors form heterotrimeric coiled coils with the N-HR of gp41, and class 4 inhibitors bind to the MPER of gp41.

the former renders neutralization by large molecules such as Abs challenging (51). In two recent papers we described a series of Fabs derived from a nonimmune phage library that bind to the N-HR in the context of both a stable N-HR trimer and a 6-HB (17, 27). The epitopes comprise a region of the N-HR that is exposed between adjacent C-HR helices in the 6-HB (Fig. 2A and B). While several of these Fabs were able to inhibit gp41-mediated cell fusion, only one, Fab 3674, was able to neutralize HIV-1 infection (17). We reasoned that the class 3 inhibitor N36$^{Mut(e,g)}$ (2) could potentiate the action of these Fabs by slowing down fusion, while the Fabs in turn could potentiate the action of N36$^{Mut(e,g)}$ by binding and therefore stabilizing the N-HR/N36$^{Mut(e,g)}$ heterotrimers. Here we show that N36$^{Mut(e,g)}$ not only enhances the activity of the neutralizing Fab 3674 but rescues neutralizing activity against resistant HIV strains and renders the series of related nonneutralizing Fabs neutralizing.

## MATERIALS AND METHODS

**Abs, cell lines, and molecular clones.** The HIV-1 expression plasmid SG3Δenv (catalogue no. 11051), the HIV-1 Env molecular clone pCAGGS SF162 gp160 (catalogue no. 10463), TZM-b1 indicator cells (JC53BL-13, catalogue no. 8129), and MAbs 2F5 (catalogue no. 1475) and 4E10 (catalogue no. 10091) were obtained from the National Institutes of Health AIDS Research and Reference Reagent Program. 293T cells were obtained from the American Type Culture Collection. The NC-1 MAb (21) was a gift from Shibo Jiang. The gp160 expression plasmid pSVIII HXBc2 was provided by J. Sodroski (22, 48). Env clones from Standard Reference Panels B (B.CAAN5342.A2, B.6535.3, B.PVO.4) (30) and C (C.ZM233M.PB6, C.DU172.17) (54) were obtained from the NIH AIDS Research Reference Reagent program (catalogue no. 11227 and 11326, respectively).

**Env-pseudotyped virus preparation.** Pseudovirus stocks were prepared essentially as described previously (23, 24). Exponentially dividing 293T cells were cotransfected using the Fugene6 transfection kit (Roche, Nutley, NJ) with the Env-deficient HIV-1 expression plasmid SG3Δenv and an Env-expressing plasmid in ratios proportional to their individual sizes (approximately 16 μg total DNA per 50 to 80% confluent T-150 culture flask). Culture supernatants were collected at 2 days posttransfection, filtered through a 0.45-μm filter, and stored at −80°C until further use.

**HIV-1 neutralization.** Env-pseudotyped HIV-1 neutralization assays were performed essentially as described previously (23, 24). Serial dilutions of peptide and Ab fusion inhibitors (10 μl) were added to Env-pseudotyped virus (in 40 μl Dulbecco modified Eagle medium plus 10% fetal calf serum), followed by addition of freshly trypsinized TZM-bl indicator cells, a HeLa-derived cell line genetically modified to constitutively express CD4, CCR5, and CXCR4 (10,000 cells in 20 μl of the same medium). After incubation at 37°C overnight, 150 μl of fresh growth medium was added to each well. At about 48 h postinfection, the cells were lysed and luciferase activity was measured using the BrightGlo luciferase assay kit (Promega) and a Wallac 1450 MicroBeta TriLux liquid scintillation and luminescence counter (Perkin-Elmer Life Sciences). Pseudovirus stocks were diluted to yield a 100- to 200-fold increase of luminescence for an infected control relative to an uninfected control. Fifty percent inhibitory concentration (IC$_{50}$s) were obtained by a nonlinear least-squares fit of the experimental data to the simple activity relationship % fusion = 100/(1 + [I]/IC$_{50}$), where [I] is the concentration of inhibitor.

**Postattachment HIV-1 neutralization assay.** The neutralizing activity of peptides and Abs was also tested after attachment of pseudovirus to the target cells following CD4 engagement. In these experiments TZM-bl cells (10$^4$ per well) were plated and allowed to adhere overnight. Plates were cooled to 4°C (a temperature at which fusion does not occur) and cold Env-pseudotyped virus was added in the same dilution as that for the regular neutralization assay. The plates were centrifuged at 4°C at 1,100 × g for 2 h, followed by washing the cells in cold medium to remove unadsorbed virus. Synchronized infection was initiated by the addition of warm medium (containing serial dilutions of peptide or Ab inhibitors). Subsequent steps in the assay were as described above for the regular neutralization assay.

**Analysis of neutralizing activity of Abs in combination with N36$^{Mut(e,g)}$ peptide.** Multiple constant-ratio combinations of Abs and synthetic N36$^{Mut(e,g)}$ peptide were tested in serial dilutions in Env-pseudotyped virus neutralization assays, as described above. Analysis of combination effects followed that of Chou and Talalay (7, 8), as described previously (16). The dose reduction index (DRI) of inhibitor x in combination with inhibitor y is given by DRI$_x$ = (IC$_{50}$)$_x$/(IC$_{50}$)$_{x,y}$, where (IC$_{50}$)$_x$ and IC$_{50}$)$_{x,y}$ are the IC$_{50}$'s of x alone and in combination with y, respectively. The combination index (CI), which describes the summation of the effects of the two inhibitors, is given by CI = (DRI$_y$)$^{-1}$ + (DRI$_y$)$^{-1}$ + (DRI$_x$·DRI$_y$)$^{-1}$, where the last term, which makes only a small contribution to CI, accounts for the state where both inhibitors are bound. CI values equal to, greater than, or less than 1 are indicative of additive, antagonistic, and synergistic effects, respectively.

**Synchronized and "time-of-addition" Env-pseudotyped HIV-1 neutralization assay.** Synchronized viral infection assays in the context of the HXB2 Env-pseudotyped virus neutralization assay were performed using the spinoculation technique (38, 42). TZM-bl cells (10$^4$ per well) were plated and allowed to
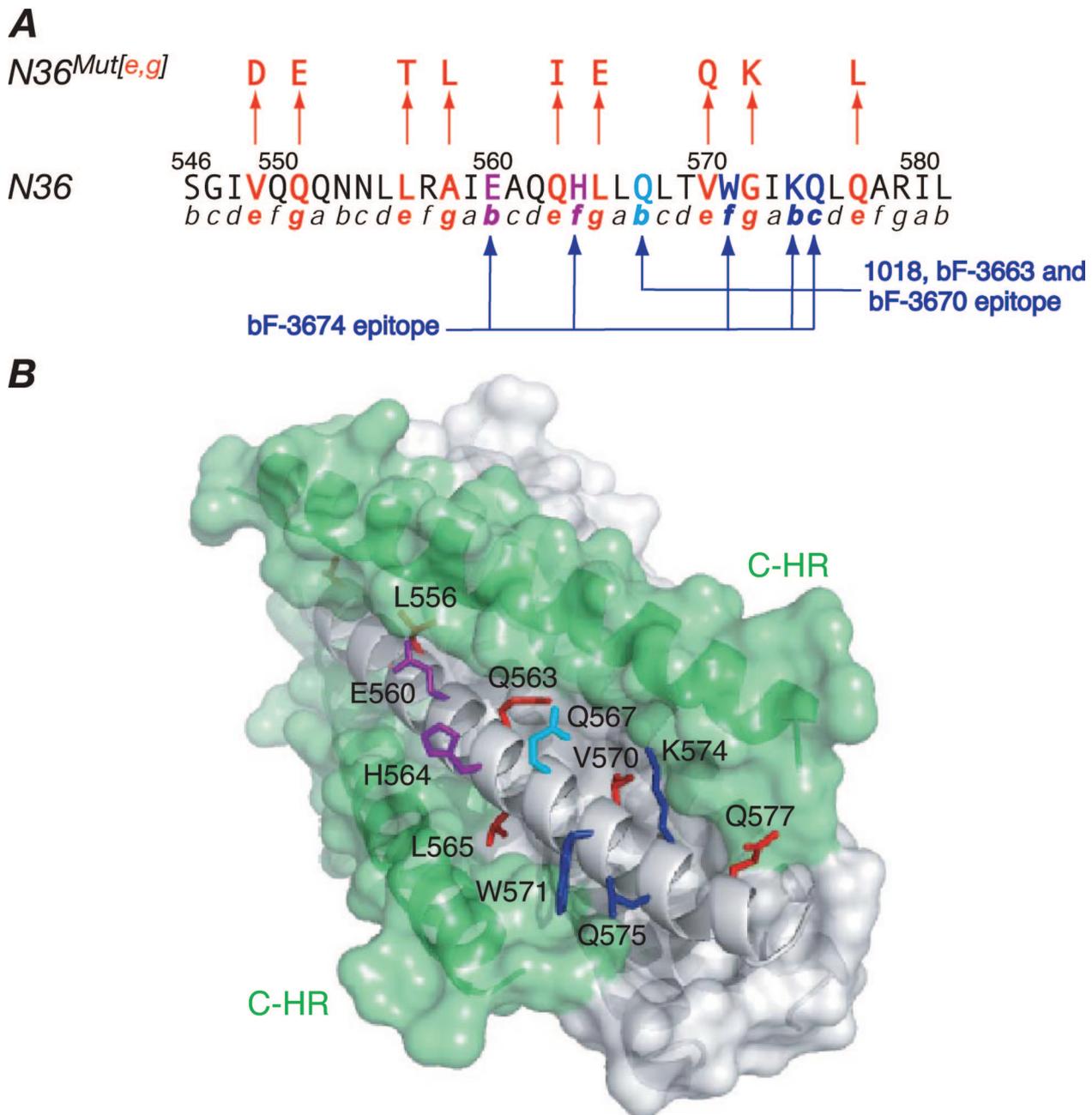
FIG. 2. N36^Mut(e,g) and the epitopes for the neutralizing (Fab 3674) and nonneutralizing (Fabs 3663, 3670, and 1018) MAbs directed against the N-HR of gp41. (A) Sequence of N36 (residues 546 to 581 of gp41), with the helical wheel positions in the N-HR trimer indicated below the sequence (5). Positions *e* and *g* (red), which contact the C-HR helix in the 6-HB conformation of gp41, are mutated in N36^Mut(e,g) (2). As a result, N36^Mut(e,g) forms a trimer that does not interact with C34 (a peptide comprising residues 628 to 661 of the C-HR of gp41) but can form heterotrimers with the N-HR of gp41, thereby inhibiting fusion (2). The epitopes of the neutralizing bF-3674 Fab (E560, H563, W571, K574, and Q575) and the nonneutralizing bF-1018, bF-3663, and bF-3670 Fabs (Q567, W571, K474, and Q575), previously delineated by alanine-scanning mutagenesis (17), are indicated. (B) Surface representation of the 6-HB core of HIV-1 gp41 (5, 49, 52). The trimeric N-HR helices are in gray, and the C-HR helices (two in the view shown) in green. Solvent-exposed N-HR residues that comprise the epitopes of the Fabs and lie in a shallow groove between two C-HR helices are shown as stick diagrams and colored as follows: residues common to the epitopes of both the neutralizing and nonneutralizing Fabs, blue; residues that are part of only the neutralizing Fab epitope, purple; the residue that is part of only the nonneutralizing Fab epitope, light blue. Residues colored in red are N-HR residues at positions *e* and *g* of the helical wheel that interact with the C-HR helices.

adhere overnight. Plates were cooled to 4°C, and cold pseudovirus was added in the same dilution as that used in the regular neutralization assay. The plates were centrifuged at 4°C at 1,100 × *g* for 2 h, and cells were washed twice with cold medium to remove unadsorbed virus and synchronize infection prior to raising

the temperature to 30 or 37°C. Fusion was initiated by addition of warm medium [containing, where indicated, a suboptimal 2 μM concentration of N36^Mut(e,g) peptide]. Fully inhibitory concentrations of inhibitor were then added at various time intervals after the initiation of synchronized infection. After 2 h, plates that
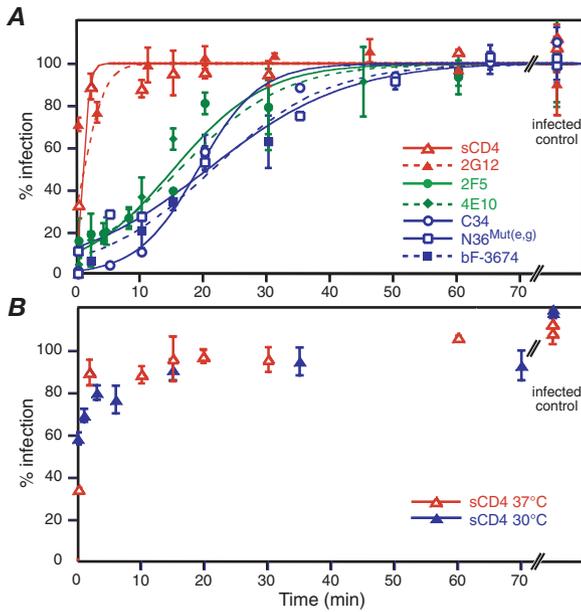
FIG. 3. Infectivity as a function of time of addition of fusion inhibitors in a synchronized HXB2-Env pseudotyped viral infectivity assay at 37°C. (A) Fully inhibitory concentrations of sCD4 (50 μg/ml), C34 (200 nM), and N36$^{Mut(e,g)}$ (50 μM) peptides and 2G12, 2F5, 4E10, and bF-3674 neutralizing MAbs (50 to 200 μg/ml) were added at the indicated time points. The experimental data (averages from four to eight experiments, with error bars representing standard deviations) were fit to a sigmoidal curve (see Materials and Methods). At 37°C, the $t_{1/2}$s of the inhibitor-sensitive state are as follows: sCD4, ≤1 min; 2G12, ≤ 1 min; 2F5, 15.0 ± 1.8; 4E10, 15.9 ± 1.7 min; C34, 19.0 ± 2.3 min; N36$^{Mut(e,g)}$, 20.6 ± 2.3 min; and bF3674, 21.5 ± 2.0 min. The so-called zero time point represents data acquired by adding cold medium containing a high concentration of inhibitor to the cold cells prior to initiating fusion by raising the temperature to 37°C. The small degree of inhibition of infection observed at the zero time point for both sCD4 and 2G12 indicates that although the pseudovirus is bound to CD4-bearing cells under these conditions, the conformational change in gp120 has not yet fully taken place in the cold and some competition with sCD4 and 2G12 is still possible. (B) Comparison of infectivity as a function of time of addition of sCD4 at 30°C and 37°C. The data for sCD4 at the two temperatures are similar.

were incubated at 30°C were transferred to 37°C. After overnight incubation at 37°C, 150 μl of fresh medium was added to each well, and luciferase activity was measured ~48 h postinfection as described above. The experimental data were fitted to a sigmoidal function given by $y = y_{max}[(1 + e^{(t_{1/2}-t)/k}]$, where $t$ is the time postinfection at which the inhibitor was added, $t_{1/2}$ is the half-life of the inhibitor-sensitive state of Env, and $k$ is a constant that determines the shape of the sigmoidal curve (42).

## RESULTS AND DISCUSSION

**Temporal window of inhibition of viral infectivity.** To assess the temporal window for viral neutralization, we examined viral infectivity as a function of time of addition of fully inhibitory concentrations of various inhibitors targeting gp120 and gp41 in a HXB2 Env-pseudotyped virus infectivity assay that is synchronized at the CD4-bound step. The results are summarized in Fig. 3. The MAb 2G12 (50) and soluble CD4 (sCD4) both bind to gp120 and are essentially inactive after CD4 engagement, with neutralization half-lives ($t_{1/2}$) of less than 1 min. The two MAbs that target the MPER of gp41, 2F5 (41) and 4E10 (47), have comparable $t_{1/2}$ values of 15.0 ± 1.8 and
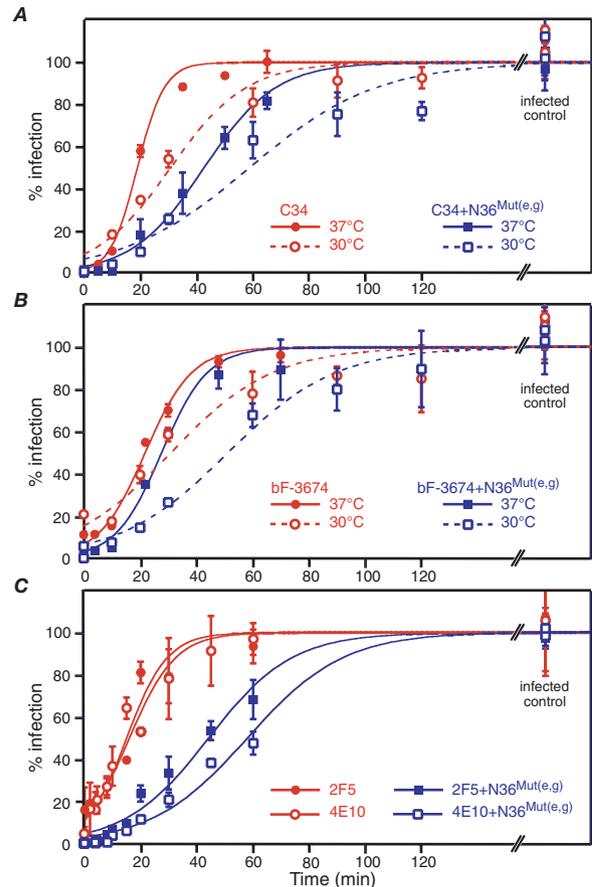
FIG. 4. Subinhibitory concentrations of N36$^{Mut(e,g)}$ increase the $t_{1/2}$ of the inhibitor-sensitive state. Viral infectivity as a function of time of addition of fully inhibitory concentrations of the C34 peptide (200 nM) (A), the neutralizing N-HR directed bF-3674 Fab (200 μg/ml) (B), and the neutralizing MPER-directed MAbs 2F5 and 4E10 (50 μg/ml) (C) in a synchronized HXB2-Env pseudotyped viral infectivity assay in the presence and absence of a subinhibitory (2 μM) concentration of N36$^{Mut(e,g)}$ is shown. The experimental data (averages from four to eight experiments, with error bars representing standard deviations) were fit to a sigmoidal curve (see Materials and Methods). The $t_{1/2}$ values for the inhibitor-sensitive state are as follows: C34 at 37°C, 19.0 ± 2.3 min; C34 plus N36$^{Mut(e,g)}$ at 37°C, 42.6 ± 1.8 min; C34 at 30°C, 34.0 ± 5.5 min; C34 plus N36$^{Mut(e,g)}$ at 30°C, 62.9 ± 6.9 min; bF-3674 at 37°C, 21.5 ± 2.0 min; bF-3674 plus N36$^{Mut(e,g)}$ at 37°C, 27.8 ± 1.8 min; bF-3674 at 30°C, 30.9 ± 6.7 min; bF-3674 plus N36$^{Mut(e,g)}$ at 30°C, 51.3 ± 4.3 min; 2F5 and 4E10 at 37°C, 15.0 ± 1.8 and 15.9 ± 1.7 min (respectively); 2F5 and 4E10 plus N36$^{Mut(e,g)}$, 44.1 ± 2.3 and 57.9 ± 2.3 min (respectively).

15.9 ± 1.7 min, respectively, slightly shorter than those of the C34 peptide (6), the N36$^{Mut(e,g)}$ peptide (2), and the bivalent Fab bF-3674 (17) which have comparable $t_{1/2}$ values of 19.0 ± 2.3 min, 21.5 ± 2.0 min, and 20.6 ± 2.3 min, respectively. We therefore conclude that the binding sites for 2G12 and sCD4 on gp120 are unavailable, either occluded or distorted, once the CD4-induced conformational changes in gp120 have occurred upon attachment of the virus to the target cell membrane via the binding of gp120 to membrane-bound CD4. The data on the gp41-directed inhibitors indicate that the N-HR is accessible to inhibitors [cf. C34, N36$^{Mut(e,g)}$, and bF-3674] for a slightly longer period of time than the MPER (cf. 2F5 and 4E10). This result is consistent with the finding that changes in exposure

TABLE 1. N36$^{\text{Mut(e,g)}}$ and neutralizing gp41-directed MAbs inhibit infectivity synergistically in an HBX2 Env-pseudotyped virus neutralization assay[a]

| Ab peptide | Ab/N36$^{\text{Mut(e,g)}}$ combination ratio | DRI (mean ± SD) | | CI (mean ± SD) |
|---|---|---|---|---|
| | | Ab | N36$^{\text{Mut(e,g)}}$ | |
| bF-3674[b] | 1:20 | 2.4 ± 0.6 | 7.4 ± 1.6 | 0.6 ± 0.2 |
| | 1:40 | 4.0 ± 0.9 | 6.4 ± 1.2 | 0.4 ± 0.2 |
| | 1:80 | 7.0 ± 1.5 | 5.6 ± 0.9 | 0.3 ± 0.1 |
| | 1:100 | 10.0 ± 2.7 | 6.4 ± 1.5 | 0.3 ± 0.1 |
| | 1:200 | 10.4 ± 2.3 | 3.3 ± 0.6 | 0.4 ± 0.1 |
| mF-3674[b] | 1:10 | 3.7 ± 1.0 | 3.5 ± 0.8 | 0.6 ± 0.2 |
| | 1:20 | 11.8 ± 2.4 | 5.5 ± 0.9 | 0.3 ± 0.1 |
| 2F5 | 1:500 | 3.4 ± 1.0 | 8.4 ± 1.6 | 0.4 ± 0.2 |
| | 1:1,000 | 8.2 ± 1.9 | 9.7 ± 1.2 | 0.2 ± 0.1 |
| 4E10 | 1:500 | 6.2 ± 1.5 | 12.7 ± 2.7 | 0.3 ± 0.1 |
| | 1:1,000 | 12.0 ± 2.6 | 12.1 ± 2.2 | 0.2 ± 0.1 |

[a] The IC$_{50}$s of the antibodies alone are as follows: bF-3674, 88 ± 14 nM; mf-3674, 603 ± 91 nM; 2F5, 3.8 ± 1.0 nM; 4E10, 6.3 ± 3.7 nM. The IC$_{50}$ for N36$^{\text{Mut(e,g)}}$ is 5.7 ± 0.5 μM.
[b] bF-3674 and mF-3674 are the bivalent and monovalent versions of Fab 3674, respectively (16).

of the MPER occur independently of the formation of the 6-HB (10).

The impact of the time window for viral neutralization by gp41-directed inhibitors can also be gauged by comparing the IC$_{50}$s in a regular HXB2 Env-pseudotyped virus neutralization assay versus a postattachment viral neutralization experiment in which virus is specifically bound to CD4 on the target cells prior to the addition of inhibitor. The rationale for the latter experiment is that membrane-bound CD4 activates HXB2 Env, thereby rendering fusion intermediates more accessible to relatively small peptide fusion inhibitors. The IC$_{50}$s for C34 and N36$^{\text{Mut(e,g)}}$ are decreased three- to fivefold in the postattachment neutralization assay relative to the regular neutralization assay [4.4 ± 0.4 nM versus 28 ± 3 nM for C34; 2.2 ± 0.8 μM versus 5.7 ± 0.5 μM for

N36$^{\text{Mut(e,g)}}$]. For large inhibitors, such as Abs, however, where accessibility to the target site is likely to be sterically limited (18) and therefore kinetically restricted (46), one would predict that a shorter time window of neutralization would result in an increase in IC$_{50}$ in the postattachment viral neutralization assay. This is exactly what is observed. The IC$_{50}$s of 2F5 and 4E10 are increased 10- to 20-fold in the postattachment neutralization assay relative to the regular neutralization assay (72 ± 12 nM versus 3.8 ± 1.0 nM for 2F5; 59 ± 11 nM versus 6.3 ± 3.7 nM for 4E10). In contrast, the IC$_{50}$ for bF-3674 is only minimally affected in the postattachment neutralization assay (129 ± 34 nM versus 88 ± 14 nM), consistent with the longer temporal window of accessibility of the N-HR relative to the MPER.

**Prolongation of the temporal window of neutralization by N36$^{\text{Mut(e,g)}}$.** We reasoned that since N36$^{\text{Mut(e,g)}}$ disrupts trimerization of the N-HR in the PHI by sequestering the N-HR into N-HR/N36$^{\text{Mut(e,g)}}$ heterotrimers (Fig. 1), subinhibitory concentrations of N36$^{\text{Mut(e,g)}}$ could potentially extend the temporal window during which virus is susceptible to neutralization by other gp41-directed inhibitors such as C34 and bF-3674, which bind to the N-HR, and 2F5 and 4E10, which target the MPER. This is indeed the case, as shown in Fig. 4. At 37°C, the $t_{1/2}$ for C34 is approximately doubled, from 19.0 ± 1.1 to 42.6 ± 1.8 min in the absence and presence of N36$^{\text{Mut(e,g)}}$, respectively (Fig. 4A); the prolongation of the $t_{1/2}$ for bF-3674 is less marked but still significant, with the $t_{1/2}$ increasing by about 30% from 21.9 ± 1.2 min to 27.7 ± 1.8 min (Fig. 4B); and for the MPER-directed MAbs 2F5 and 4E10, the $t_{1/2}$ is increased three- to fourfold (from 15.0 ± 1.8 to 44.1 ± 2.3 min and from 15.9 ± 1.7 to 57.9 ± 2.3 min, respectively) (Fig. 4C). Reducing the temperature to 30°C, which lowers the overall rate of fusion, makes the effect for bF-3674 more pronounced, with the $t_{1/2}$ increasing by about 66% from 30.9 ± 6.7 min to 51.3 ± 4.3 min. (Fig. 4B). For C34, both $t_{1/2}$ values are proportionately increased at the lower temperature (Fig. 4A).

**Synergistic viral neutralization by bF-3674 and N36$^{\text{Mut(e,g)}}$.** The primary epitope for bF-3674 comprises the region of the

TABLE 2. N36$^{\text{Mut(e,g)}}$ enhances activity of gp41 NHR-directed MAbs, rendering nonneutralizing Abs neutralizing and rescuing neutralizing activity against resistant viruses

| Ab vs pseudovirus | Ab/N36$^{\text{Mut(e,g)}}$ combination ratio | IC$_{50}$ in combination (mean ± SD) | | Individual IC$_{50}$ (mean ± SD) | |
|---|---|---|---|---|---|
| | | Ab (nM) | N36$^{\text{Mut(e,g)}}$ (μM) | Ab (nM) | N36$^{\text{Mut(e,g)}}$ (μM) |
| bF-3674 vs SF162 | 1:20 | 140 ± 10 | 3.1 ± 0.2 | 786 ± 67 | NA[a] |
| | 1:40 | 106 ± 29 | 4.7 ± 1.3 | | |
| mF-3674 vs SF162 | 1:10 | 481 ± 250 | 4.8 ± 2.5 | NA | NA |
| | 1:20 | 300 ± 130 | 6.0 ± 2.5 | | |
| | 1:40 | 240 ± 70 | 9.5 ± 2.9 | | |
| bF-3670 vs HXB2 | 1:20 | 62 ± 9 | 1.3 ± 0.3 | NA | 5.7 ± 0.5 |
| | 1:40 | 35 ± 11 | 1.4 ± 0.4 | | |
| bF-3663 vs HXB2 | 1:20 | 89 ± 14 | 1.8 ± 0.6 | NA | 5.7 ± 0.5 |
| | 1:40 | 35 ± 10 | 1.4 ± 0.4 | | |
| bF-1018 vs HXB2 | 1:20 | 330 ± 130 | 1.8 ± 0.6 | NA | 5.7 ± 0.5 |
| bF-1018 vs SF162 | 1:20 | 460 ± 120 | 10 ± 3 | NA | NA |

[a] NA, no detectable neutralizing activity in the range of concentrations tested [up to 1 μM for the bivalent Fabs, up to 2 μM for the monovalent Fab, and up to 20 μM for N36$^{\text{Mut(e,g)}}$].
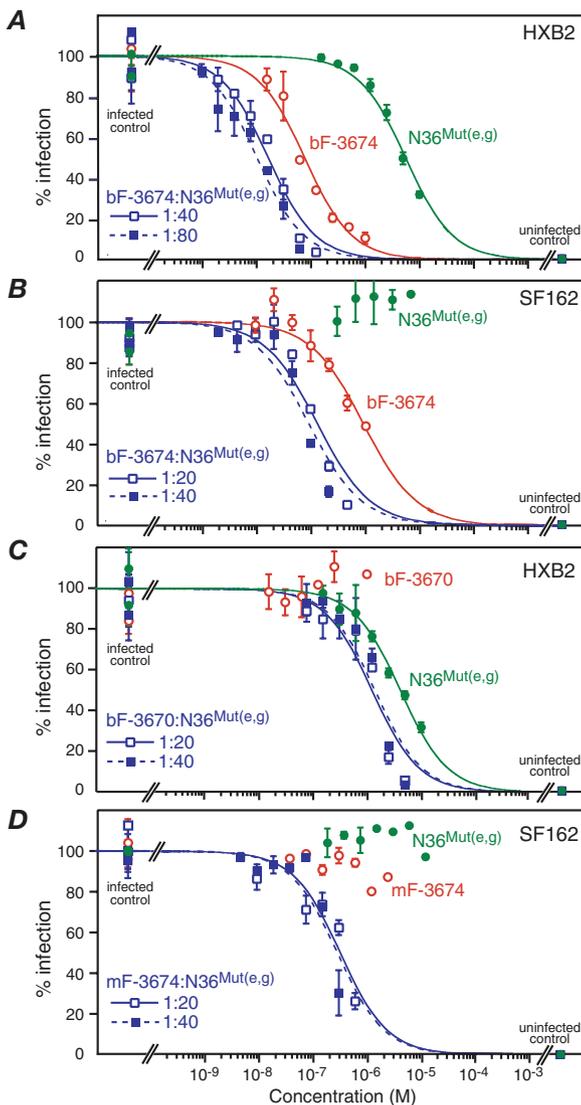
FIG. 5. N36$^{Mut(e,g)}$ displays synergistic antiviral activity with both neutralizing and nonneutralizing Fabs directed against the N-HR of gp41. Dose-response curves for antiviral activity of N36$^{Mut(e,g)}$ alone (green), Fab alone (red), and Fab + N36$^{Mut(e,g)}$ in two fixed combination ratios (blue) against HXB2 (A and C) and SF162 (B and D) Env-pseudotyped viruses are shown. The Fabs are bF-3674 in panels A and B, bF-3670 in panel C, and mF-3674 in panel D. The concentrations for the combination curves in panels A, B, and D refer to the concentration of Fab, while in panel C they refer to the concentration of N36$^{Mut(e,g)}$. The experimental data (averages from six to eight experiments, with error bars representing standard deviations) are fit by nonlinear least-squares minimization to a simple binding isotherm given by % infection = 100/(1 + [I[]/IC$_{50}$), where [I] is the concentration of fusion inhibitor. IC$_{50}$s, DRIs, and CIs are provided in Tables 1 and 2.
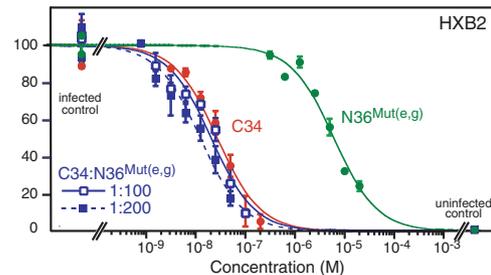


FIG. 6. N36$^{Mut(e,g)}$ and C34 peptides inhibit infectivity additively in an HXB2 Env-pseudotyped virus neutralization assay. Dose-response curves for antiviral activity of N36$^{Mut(e,g)}$ alone (green), C34 alone (red), and C34 plus N36Mut$^{(e,g)}$ in two combination ratios, 1:100 and 1:200, are shown. The concentrations for the combination curves refer to the concentration of C34. The experimental data (averages of two measurements, with error bars representing standard deviations) are fit by nonlinear least-squares minimization to a simple binding isotherm (see the Fig. 5 legend). For this data set, the IC$_{50}$s for C34 and N36$^{Mut(e,g)}$ alone are 27.5 ± 5.2 nM and 6.2 ± 0.8 μM, respectively. The DRIs for C34 and N36$^{Mut(e,g)}$ in a combination ratio of 1:100 are 1.3 ± 0.3 and 3.0 ± 0.7, respectively, giving a CI of 1.3 ± 0.5. The corresponding values at a combination ratio of 1:200 are 2.2 ± 0.6, 2.5 ± 0.5, and 1.1 ± 0.4, respectively. Thus, in this combination ratio range, the average CI is 1.2 ± 0.4, indicative of additive inhibition.

mers. This, together with the results in the previous section, suggested to us that bF-3674 and N36$^{Mut(e,g)}$ could neutralize HIV-1 synergistically. The results are summarized in Tables 1 and 2 and Fig. 5.

Optimal synergy should be obtained when the ratio of the two inhibitors is approximately equal to the ratio of their individual IC$_{50}$'s (see footnote *a* to Table 1). Synergy is assessed by the value of the CI, for which values of about 1, less than 1, and greater than 1 are indicative of additive, synergistic, and antagonistic effects, respectively (see Materials and Methods) (7, 8, 16). HXB2 Env-pseudotyped virus neutralization assays using fixed combination ratios of N36$^{Mut(e,g)}$ with either bF-3674 or mF-3674 (the bivalent and monovalent version of Fab 3674, respectively) show CIs of 0.3 to 0.6 over a range of combination ratios, clearly indicating synergistic inhibition (Table 2 and Fig. 5A), as predicted above.

The two MAbs that target the MPER, 2F5 and 4E10, also neutralize HXB2 synergistically with N36$^{Mut(e,g)}$, with CI values of 0.2 to 0.3 (Table 2). This effect is readily explained, since these two classes of inhibitors act at distinct sites on gp41 (Fig. 1). Similarly, N36$^{Mut(e,g)}$ and the class 2 inhibitor N$_{CCG}$-gp41, which targets the C-HR, also neutralize synergistically with a CI value of 0.5 to 0.6 (16). The formation of N-HR/N36$^{Mut(e,g)}$ heterotrimers will enhance the probability of 2F5/4E10 binding to the MPER and of N$_{CCG}$-gp41 binding to the C-HR. Conversely, binding of 2F5/4E10 and N$_{CCG}$-gp41 to their target site on gp41 will enhance the probability of N-HR/N36$^{Mut(e,g)}$ heterotrimer formation. The net result is that the probability of 6-HB formation is greatly diminished by the combination of N36$^{Mut(e,g)}$ with either class 2 or class 4 inhibitors. This result is fully consistent with the three- to fourfold increase in the temporal window for viral neutralization by 4E10 and 2F5 in the presence of N36$^{Mut(e,g)}$ (Fig. 4C).

By way of contrast, the HXB2 neutralization activity of the C34 peptide (IC$_{50}$ = 28 ± 5 nM) is additive with that of N36$^{Mut(e,g)}$, with an average CI of 1.2 ± 0.4 in combination

N-HR trimer located between two C-HR helices that remains exposed in the context of the 6-HB (Fig. 2) (17). Thus, the binding site for bF-3674 is distinct from that for the C-HR or C34 peptide (3, 5, 6, 49, 52). The sequence of N36$^{Mut(e,g)}$ differs from that of the N-HR in that the residues that interact with the C-HR have been mutated (2). Consequently, the bF-3674 epitope remains intact in N-HR/N36Mut$^{(e,g)}$ heterotri-

TABLE 3. N36$^{Mut(e,g)}$ and Fab bF-3674 neutralize contemporary primary isolates of subtype B and C clades of HIV-1 synergistically[a]

| Pseudovirus | bF-3674/N36$^{Mut(e,g)}$ combination ratio | IC$_{50}$ in combination (mean ± SD) | | Individual IC$_{50}$ (mean ± SD) | | DRI (mean ± SD) | | CI (mean ± SD) |
|---|---|---|---|---|---|---|---|---|
| | | bF-3674 (nM) | N36$^{Mut(e,g)}$ (μM) | bF-3674 (nM) | N36$^{Mut(e,g)}$ (μM) | bF-3674 | N36$^{Mut(e,g)}$ | |
| B.CAAN5342.A2 | 1:20 | 72 ± 7 | 1.4 ± 0.1 | 310 ± 60 | 41 ± 7 | 4.3 ± 1.0 | 28 ± 5 | 0.3 ± 0.1 |
| | 1:40 | 59 ± 4 | 2.4 ± 0.1 | | | 5.3 ± 1.1 | 17 ± 3 | 0.3 ± 0.1 |
| B.6535.3 | 1:20 | 120 ± 17 | 2.5 ± 0.3 | 2840 ± 820 | 7.1 ± 1.1 | 24 ± 8 | 2.9 ± 0.6 | 0.4 ± 0.2 |
| | 1:40 | 70 ± 12 | 2.8 ± 0.5 | | | 41 ± 14 | 2.6 ± 0.6 | 0.4 ± 0.2 |
| B.PVO.4 | 1:20 | 730 ± 210 | 15 ± 4 | NA[b] | 59 ± 17 | | 4.0 ± 1.6 | —[c] |
| | 1:40 | 280 ± 70 | 11 ± 3 | | | | 5.3 ± 2.0 | —[c] |
| C.ZM233M.PB6 | 1:20 | 12 ± 1 | 0.2 ± 0.0 | 44 ± 10 | 11 ± 4 | 3.8 ± 0.9 | 46 ± 17 | 0.3 ± 0.2 |
| | 1:40 | 9 ± 2 | 0.4 ± 0.1 | | | 5.2 ± 1.5 | 31 ± 13 | 0.2 ± 0.1 |
| C.DU172.17 | 1:20 | 27 ± 4 | 0.6 ± 0.1 | 70 ± 13 | 4.6 ± 1.0 | 2.6 ± 0.7 | 8.4 ± 2.3 | 0.6 ± 0.2 |
| | 1:40 | 18 ± 3 | 0.7 ± 0.1 | | | 4.0 ± 1.0 | 6.4 ± 1.7 | 0.5 ± 0.2 |

[a] Envelope clones from standard reference panel B (B.CAAN5342.A2, B.6535.3, and B.PVO.4) (30) and C (C.ZM233M.PB6 and C.DU172.17) (34) were used to produce the Env-pseudotyped HIV-1.
[b] NA, no detectable neutralizing activity in the range of concentrations tested [up to 1 μM for bF-3674 and 20 μM for N36$^{Mut(e,g)}$].
[c] A combination index could not be obtained since Fab-3674 displayed no detectable neutralizing activity on its own (see footnote b).

ratios of 1:100 and 1:200 (Fig. 6). This is due to the fact that C34 binds to two adjacent N-HR helices in the trimer, and hence the heterotrimeric state comprising two N-HR helices and one N36$^{Mut(e,g)}$ helix, [N-HR]$_2$/[N36$^{Mut(e,g)}$], will only have a single C34 binding site, compared to three for the native N-HR trimer, while the [N-HR]/[N36$^{Mut(e,g)}$]$_2$ heterotrimer will have no available binding site for C34. The same is true for the recently described neutralizing MAb 8K8, which binds to the N-HR only in the context of a fully exposed N-HR trimer but not as the 6-HB (37). Hence, the 8K8 epitope on the N-HR trimer shares residues in common with the binding site for the C-HR and C34 peptide. The IC$_{50}$ for 8K8 alone is 400 ± 54 nM, and the CI for 8K8 and N36$^{Mut(e,g)}$ in combination is 0.9 ± 0.2.

**Rescuing neutralization activity of Fabs directed against the N-HR by N36$^{Mut(e,g)}$.** The epitope for the nonneutralizing bF-3670, bF-3663, and bF-1018 Fabs (17, 27) is very similar to that of bF-3674 but is shifted by about one helical turn (17) (Fig. 2). Presumably the absence of neutralizing activity for these three Fabs on their own is due to a combination of reduced affinity for their N-HR epitope in the PHI and reduced accessibility of this epitope relative to that for bF-3674. We examined the mutually synergistic effects of these Fabs and N36$^{Mut(e,g)}$ in neutralization of both HXB2 and SF162 Env-pseudotyped viruses. CIs could not be determined, since at least one of the inhibitors was nonneutralizing on its own.

Fabs bF-3670, bF-3663, and bF-1018 do not neutralize HXB2 on their own but reduce the IC$_{50}$ of N36$^{Mut(e,g)}$ three- to fourfold (Fig. 5C and Table 3). N36$^{Mut(e,g)}$ fails to neutralize SF162 on its own but decreases the IC$_{50}$ for bF-3674 by five- to sevenfold (Fig. 5B and Table 3). Both mF-3674 and bF-1018 fail to neutralize SF162, but in the presence of N36$^{Mut(e,g)}$ neutralization activity is observed (Table 3 and Fig. 5D). (Note that the difference in neutralization activity between the bivalent bF-3674 Fab and the monovalent mF-3674 Fab is almost certainly a consequence of the increased avidity of bF-3674 owing to its bivalent nature.)

The MAb NC-1, raised against the 6-HB in the form of a minimal ectodomain gp41 core (21), fails to inhibit infectivity in the Env-pseudotyped virus neutralization assay and does not enhance the inhibitory activity of N36$^{Mut(e,g)}$ (data not shown). These data indicate that while NC-1 binds to the 6-HB with high affinity, its affinity for the PHI is low, consistent with Western blot data (9). Once 6-HB formation has occurred, the path to fusion is essentially irreversible. Since N36$^{Mut(e,g)}$ acts only on the PHI and cannot bind to the 6-HB, it is not surprising that NC-1 remains nonneutralizing in the presence of N36$^{Mut(e,g)}$. These findings are fully consistent with the observation that N36$^{Mut(e,g)}$ reduces the apparent binding of NC-1 to gp41 during the course of cell-cell fusion (9).

**Synergistic neutralization of primary HIV-1 isolates by bF-3674 and N36$^{Mut(e,g)}$.** To test whether the synergistic neutralization of HIV-1 by bF-3674 and N36$^{Mut(e,g)}$ observed for laboratory-adapted strains of HIV-1 extended to primary isolates, we carried out a series of combination Env-pseudotyped virus neutralization assays with Env from three B-clade and two C-clade strains obtained from standard reference panels B and C, respectively. The results are summarized in Fig. 7 and Table 3. In each case, synergistic inhibition of infectivity is observed, with CI values ranging from 0.2 to 0.6 (Table 3). Further, in the case of strain B.PVO.4, where no neutralizing activity is observed for bF-3674 alone and only low neutralizing activity is observed for N36$^{Mut(e,g)}$ (IC$_{50}$, ~60 μM), clear-cut neutralization activity is observed when bF-3674 and N36$^{Mut(e,g)}$ are combined in ratios of 1:20 and 1:40, with DRIs of 4 to 5 for N36$^{Mut(e,g)}$ [i.e., the IC$_{50}$ is reduced to 11 to 15 μM as expressed in terms of N36$^{Mut(e,g)}$ concentration] (Fig. 7B and Table 3).

**Synergistic neutralization by bF-3674 and sCD4.** sCD4 is known to trigger conformational changes in gp120 leading to the exposure of gp41 and the formation of the PHI (14, 32, 35). This effect of sCD4 has previously been used to reveal cryptic epitopes on gp120 and gp41 and to render them accessible to targeting by peptides and Abs (27, 45). We therefore reasoned that sCD4 might also potentiate the neutralizing activity of Fab
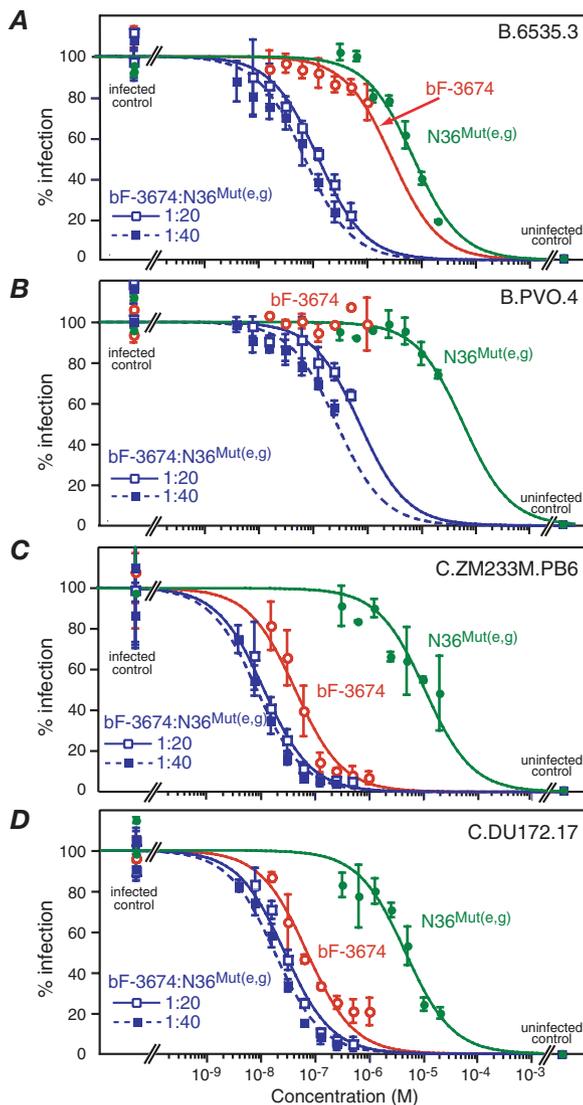
FIG. 7. N36$^{Mut(e,g)}$ and Fab bF-3674 display synergistic antiviral activity against primary B and C subtype HIV-1 isolates in the Env-pseudotyped virus neutralization assay. Dose-response curves for antiviral activity of N36$^{Mut(e,g)}$ alone (green), bF-3674 alone (red), and bF-3674 plus N36$^{Mut(e,g)}$ in two fixed combination ratios (blue) against Env-pseudotyped viruses from B (A and B) and C (C and D) clades are shown. The concentrations for the combination curves refer to the concentration of Fab-3674. The experimental data are fit by nonlinear least-squares minimization to a simple binding isotherm given by % infection = $100/(1 + [I[]/IC_{50})$, where [I] is the concentration of fusion inhibitor. IC$_{50}$s, DRIs, and CIs are provided in Table 3.

bF-3674. The results are summarized in Table 4, which clearly show that sCD4 inhibits infectivity in an HBX2 Env-pseudotyped virus neutralization assay synergistically with bF-3674 (CI of ~0.4 to 0.6), 2F5 (CI of ~0.1 to 0.2), and 4E10 (CI of ~0.3). While the underlying mechanism of synergistic neutralization with sCD4 is clearly different from that with N36$^{Mut(e,g)}$, both sCD4 and N36$^{Mut(e,g)}$ clearly increase the probability of binding bF-3674, 2F5, and 4E10 Abs to the PHI of gp41, either by inducing the early and prolonged appearance of the PHI in the case of sCD4 or by sequestering the PHI into heterotrimers in the case of N36$^{Mut(e,g)}$.

TABLE 4. sCD4 and neutralizing gp41-directed MAbs inhibit infectivity synergistically in an HBX2 Env-pseudotyped virus neutralization assay[a]

| Ab | Ab/sCD4 Combination ratio | DRI (mean ± SD) | | CI (mean ± SD) |
|---|---|---|---|---|
| | | Ab | sCD4 | |
| bF-3674 | 10:1 | 2.5 ± 0.7 | 11.8 ± 3.7 | 0.5 ± 0.3 |
| | 20:1 | 3.1 ± 1.0 | 30.2 ± 8.6 | 0.4 ± 0.2 |
| | 40:1 | 1.7 ± 0.5 | 45.3 ± 10.6 | 0.6 ± 0.3 |
| 2F5 | 1:5 | 9.6 ± 2.7 | 11.0 ± 3.3 | 0.2 ± 0.1 |
| | 1:10 | 22.4 ± 8.7 | 12.9 ± 5.0 | 0.13 ± 0.08 |
| 4E10 | 1:5 | 9.7 ± 2.6 | 5.9 ± 1.9 | 0.3 ± 0.1 |
| | 1:10 | 17.5 ± 3.2 | 5.2 ± 1.3 | 0.3 ± 0.1 |

[a] The IC$_{50}$s of the antibodies alone are as follows: bF-3674, 88 ± 14 nM; 2F5, 3.8 ± 1.0 nM; 4E10, 6.3 ± 3.7 nM. The IC$_{50}$ for sCD4 is 27.2 ± 4.9 nM.

**Concluding remarks.** In this paper we have shown that various HIV-1-neutralizing inhibitors that target the N-HR of gp41 exhibit very similar lifetimes for the inhibitory-sensitive state and that these lifetimes are slightly longer than those of the MPER-directed MAbs 4E10 and 2F5 (Fig. 3). The temporal window for viral neutralization can be significantly extended by the class 3 inhibitor N36$^{Mut(e,g)}$ (Fig. 4), which sequesters the PHI through the formation of heterotrimers with the N-HR of gp41 (Fig. 1). Moreover, we have shown that N36$^{Mut(e,g)}$ potentiates the neutralizing activity of 4E10 and 2F5, as well as that of a series of Fabs whose epitope comprises the region of the N-HR that remains exposed between the C-HR helices in the 6-HB (Fig. 2B). The neutralizing activity of Fab bF-3674 against both laboratory-adapted strains (HXB2 and SF162) and primary isolates obtained from the standard B (30) and C (54) subtype reference panels is enhanced, neutralizing activity against resistant strains is reestablished (cf. mF3672 against SF162 and bF3674 against B.PVO.4), and non-neutralizing Fabs are rendered neutralizing (cf. bF-3670, bF-3663, and bF-1018) (Tables 1 and 2 and Fig. 5). These data suggest that N36$^{Mut(e,g)}$ may potentially be able to enhance the anti-HIV potency of the gp41-directed immune response by converting some of the nonneutralizing or very weakly neutralizing N-HR gp41-directed Abs found in patient sera (39) to neutralizing Abs and may also represent a potentially useful adjunct in treatment of AIDS with gp41-directed neutralizing MAbs.

**REFERENCES**

1. **Berger, E. A., P. M. Murphy, and J. M. Farber.** 1999. Chemokine receptors as HIV-1 coreceptors: roles in viral entry, tropism and disease. Annu. Rev. Immun. **17:**657–700.
2. **Bewley, C. A., J. M. Louis, R. Ghirlando, and G. M. Clore.** 2002. Design of a novel peptide inhibitor of HIV fusion that disrupts the internal trimeric coiled-coil of gp41. J. Biol. Chem. **277:**14238–14245.
3. **Caffrey, M., M. Cai, J. Kaufman, S. J. Stahl, P. T. Wingfield, D. G. Covell, A. M. Gronenborn, and G. M. Clore.** 1998. Three-dimensional solution structure of the 44 kDa ectodomain of SIV gp41. EMBO J. **17:**4572–4584.

4. **Chan, D. C., and P. S. Kim.** 1998. HIV entry and its inhibition. Cell **93:**681–684.

5. **Chan, D. C., D. Fass, J. M. Berger, and P. S. Kim.** 1997. Core structure of gp41 from the HIV envelope glycoprotein. Cell **89:**263–273.

6. **Chan, D. C., C. T. Chutkowski, and P. S. Kim.** 1998. Evidence that a prominent cavity in the coiled-coil of HIV type 1 gp41 is an attractive drug target. Proc. Natl. Acad. Sci. USA **95:**15613–15617.

7. **Chou, T. C., and P. Talalay.** 1981. Generalized equations for the analysis of inhibitions of Michaelis-Menten and higher-order kinetic systems for two or more mutually exclusive and non-exclusive inhibitors. Eur. J. Biochem. **115:**207–216.

8. **Chou, T. C., and P. Talalay.** 1984. Quantitative analysis of dose-effect relationships: the combined effects of multiple drugs or enzyme inhibitors. Adv. Enzyme Regul. **22:**27–55.

9. **Dimitrov, A. S., J. M. Louis, C. A. Bewley, G. M. Clore, and R. Blumenthal.** 2005. Conformational changes in HIV-1 gp41 in the course of HIV-1 envelope glycoprotein-mediated fusion and inactivation. Biochemistry **44:**12471–12479.

10. **Dimitrov, A. S., A. Jacobs, C. M. Finnegan, G. Stiegler, H. Katinger, and R. Blumenthal.** 2007. Exposure of the membrane-proximal external region of HIV-1 gp41 in the course of HIV-1 envelope glycoprotein-mediated fusion. Biochemistry **46:**1398–1401.

11. **Eckert, D. M., and P. S. Kim.** 2001. Mechanisms of viral membrane fusion and its inhibition. Annu. Rev. Biochem. **70:**777–810.

12. **Eckert, D. M., and P. S. Kim.** 2001. Design of potent inhibitors of HIV-1 entry from the gp41 N-peptide region. Proc. Natl. Acad. Sci. USA **98:**11187–11192.

13. **Eckert, D. M., V. N. Malashkevich, L. H. Hong, P. A. Carr, and P. S. Kim.** 1999. Inhibiting HIV-1 entry: discovery of D-peptide inhibitors that target the gp41 coiled-coil pocket. Cell **99:**103–115.

14. **Furuta, R. A., C. T. Wild, Y. Weng, and C. D. Weiss.** 1998. Capture of an early fusion-active conformation of HIV-1 gp41. Nature Struct. Biol. **5:**276–279.

15. **Golding, H., M. Zaitseva, E. de Rosny, L. R. King, J. Manischewitz, I. Sidorov, M. K. Gorny, S. Zolla-Pazner, D. S. Dimitrov, and C. D. Weiss.** 2002. Dissection of human immunodeficiency virus type 1 entry with neutralizing antibodies to gp41 fusion intermediates. J. Virol. **76:**6780–6790.

16. **Gustchina, E., J. M. Louis, C. A. Bewley, and G. M. Clore.** 2006. Synergistic inhibition of HIV-1 envelope-mediated membrane fusion by inhibitors targeting the N- and C-terminal heptad repeats of gp41. J. Mol. Biol. **364:**283–289.

17. **Gustchina, E., J. M. Louis, S. N. Lam, C. A. Bewley, and G. M. Clore.** 2007. A monoclonal Fab derived from a human nonimmune phage library reveals a new epitope on gp41 and neutralizes diverse human immunodeficiency virus type 1 strains. J. Virol. **81:**12946–12953.

18. **Hamburger, A. E., S. Kim, R. B. Welch, and M. S. Kay.** 2005. Steric accessibility of the HIV-1 gp41 N-trimer region. J. Biol. Chem. **280:**12567–12572.

19. **Jacobs, A., H. Garg, M. Viard, Y. Raviv, A. Puri, and R. Blumenthal.** 2008. HIV-1 envelope glycoprotein-mediated fusion and pathogenesis: implications for therapy and vaccine development. Vaccine **26:**3026–3035.

20. **Jiang, S., K. Lin, N. Strick, and A. R. Neurath.** 1993. HIV-1 inhibition by a peptide. Nature **365:**113.

21. **Jiang, S., K. Lin, and M. Lu.** 1998. A conformation specific monoclonal antibody reacting with fusion-active gp41 from human immunodeficiency virus type I envelope glycoprotein. J. Virol. **72:**10213–10217.

22. **Karlsson, G. B., F. Gao, J. Robinson, B. Hahn, and J. Sodroski.** 1996. Increased envelope spike intensity and stability are not required for the neutralization of primary human immunodeficiency viruses. J. Virol. **70:**6136–6142.

23. **Li, M., F. Gao, J. R. Mascola, L. Stamatatos, V. R. Polonis, M. Koutsoukos, G. Voss, P. Goepfert, P. Gilbert, K. M. Greene, M. Bilska, D. L. Kothe, J. F. Salazar-Gonzalez, X. Wei, J. M. Decker, B. H. Hahn, and D. C. Montefiori.** 2005. Human immunodeficiency virus type 1 env clones from acute and early subtype B infections for standardized assessments of vaccine-elicited neutralizing antibodies. J. Virol. **79:**10108–10125.

24. **Li, Y., K. Svehla, N. L. Mathy, G. Voss, J. R. Mascola, and R. Wyatt.** 2006. Characterization of antibody responses elicited by human immunodeficiency virus type 1 primary isolate trimeric and monomeric envelope glycoproteins in selected adjuvants. J. Virol. **80:**1414–1426.

25. **Louis, J. M., C. A. Bewley, and G. M. Clore.** 2001. Design and properties of $N_{CCG}$-gp41, a chimeric gp41 molecule with nanomolar HIV-1 fusion inhibitory activity. J. Biol. Chem. **276:**29485–29489.

26. **Louis, J. M., G. M. Clore, and C. A. Bewley.** 2003. Covalent trimers of the internal N-terminal trimeric coiled-coil of gp41 and antibodies directed against them are potent inhibitors of HIV envelope-mediated cell fusion. J. Biol. Chem. **278:**20278–20285.

27. **Louis, J. M., C. A. Bewley, E. Gustchina, A. Aniana, and G. M. Clore.** 2005. Characterization and HIV-1 fusion inhibitory properties of monoclonal Fabs obtained from a human non-immune phage library selected against diverse epitopes of the ectodomain of HIV-1 gp41. J. Mol. Biol. **353:**945–951.

28. **Lu, M., S. C. Blacklow, and P. S. Kim.** 1995. A trimeric structural domain of the HIV-1 transmembrane glycoprotein. Nat. Struct. Biol. **2:**1075–1082.

29. **Luftig, M. A., M. Mattu, P. Di Giovine, R. Geleziunas, R. Hrin, G. Barbato, E. Bianchi, M. D. Miller, A. Pessi, and A. Carfi.** 2006. Structural basis for HIV-1 neutralization by a gp41 fusion intermediate-directed antibody. Nat. Struct. Mol. Biol. **13:**740–747.

30. **Mascola, J. R., P. D'Souza, P. Gilbert, B. H. Hahn, N. L. Haigwood, L. Morris, C. J. Petropoulos, V. R. Polonis, M. Sarzotti, and D. C. Montefiori.** 2005. Recommendations for the design and use of standard virus panels to assess neutralizing antibody responses elicited by candidate human immunodeficiency virus type 1 vaccines. J. Virol. **79:**10103–10107.

31. **Matthews, T., M. Salgo, M. Greenberg, J. Chung, R. DeMasi, and C. Bolognesi.** 2004. Enfuvirtide: the first therapy to inhibit the entry of HIV-1 into host CD4 lymphocytes. Nat. Rev. Drug Disc. **3:**215–225.

32. **Melikyan, G. B., R. M. Markosyan, H. Hemmati, M. K. Demedico, D. M. Lamvert, and F. S. Cohen.** 2000. Evidence that the transition of HIV-1 gp41 into a six-helix bundle, not the bundle conformation, induces membrane fusion. J. Cell Biol. **151:**413–423.

33. **Melikyan, G. B., M. Egelhofer, and D. von Laer.** 2006. Membrane-anchored inhibitory peptides capture human immunodeficiency virus type 1 gp41 conformations that engage the target membrane prior to fusion. J. Virol. **80:**3249–3258.

34. **Miller, M. D., R. Geleziunas, E. Bianchi, S. Lennard, R. Hrin, H. Zhang, M. Lu, Z. An, P. Ingallinella, M. Finotto, M. Mattu, A. C. Finnefrock, D. Bramhill, J. Cook, D. M. Eckert, R. Hampton, M. Patel, S. Janatow, J. Joyce, G. Ciliberto, R. Cortese, P. Lu, W. Strohl, W. Schleif, M. McElhaugh, S. Lane, C. Lloyd, D. Lowe, J. Osbourn, T. Vaughan, E. Emini, G. Barbato, P. S. Kim, D. J. Hazua, J. W. Shiver, and A. Pessi.** 2005. A human monoclonal antibody neutralizes diverse HIV-1 isolates by binding a critical gp41 epitope. Proc. Natl. Acad. Sci. USA **102:**14759–14764.

35. **Moore, J. P., J. A. McKeating, R. A. Weiss, and Q. J. Sattentau.** 1990. Dissociation of gp120 from HIV-1 virions induced by soluble CD4. Science **250:**1139–1142.

36. **Muster, T., F. Steindl, M. Purtscher, A. Trkola, A. Klima, G. Himmler, F. Ruker, and H. Katinger.** 1993. A conserved neutralizing epitope on gp41 of human immunodeficiency virus type 1. J. Virol. **67:**6642–6647.

37. **Nelson, J. D., H. Kinkead, F. M. Brunel, D. Leaman, R. Jensen, J. M. Louis, T. Maruyama, C. A. Bewley, K. Bowdish, G. M. Clore, P. E. Dawson, S. Frederickson, R. G. Mage, D. G. Richman, D. R. Burton, and R. Zwick.** 2008. Antibody elicited against the gp41 N-heptad repeat (NHR) coiled-coil can neutralize HIV-1 with modest potency but non-neutralizing antibodies also bind to NHR mimetics. Virology [Epub ahead of print.] doi:10.1016/j.virol.2008.04.005.

38. **O'Doherty, U., W. J. Swiggard, and M. H. Malim.** 2000. A sensitive quantitative assay for human immunodeficiency virus type 1 integration. J. Virol. **74:**10074–10080.

39. **Penn-Nicholson, A., D. P. Han, S. J. Kim, H. Park, R. Ansari, D. C. Montefiori, and M. W. Cho.** 2008. Assessment of antibody responses against gp41 in HIV-1-infected patients using soluble gp41 fusion proteins and peptides derived from M group consensus envelope. Virology **373:**442–456.

40. **Prabakaran, P., A. S. Dimitrov, T. R. Fouts, and D. S. Dimitrov.** 2007. Structure and function of the HIV envelope glycoprotein as entry mediator, vaccine immunogen and target for inhibitors. Adv. Pharmacol. **55:**33–97.

41. **Purtscher, M., A. Trkola, A., G. Gruber, A. Buchacher, R. Predl, F. Steindl, C. Tauer, R. Berger, N. Barrett, A. Junbauer, and H. Katinger.** 1994. A broadly neutralizing human nonclonal antibody against gp41 of human immunodeficiency virus type 1. AIDS Res. Hum. Retroviruses **10:**1651–1658.

42. **Reeves, J. D., S. A. Gallo, N. Ahmad, J. L. Miamidian, P. E. Harvey, M. Sharron, S. Pohlmann, J. N. Sfakianos, C. A. Derdeyn, R. Blumenthal, E. Hunter, and R. W. Doms.** 2002. Sensitivity of HIV-1 to entry inhibitors correlates with envelope/coreceptor affinity, receptor density and fusion kinetics. Proc. Natl. Acad. Sci. USA **99:**16249–16254.

43. **Root, M. J., and H. K. Steger.** 2004. HIV-1 gp41 as a target for viral entry inhibition. Curr. Pharm. Design. **10:**1805–1825.

44. **Root, M. J., and M. S. Kay, and P. S. Kim.** 2001. Protein design of an HIV-1 entry inhibitor. Science **291:**884–888.

45. **Salzwedel, K., E. D. Smith, B. Dey, and E. A. Berger.** 2000. Sequential CD4-coreceptor interactions in human immunodeficiency virus type 1 Env function: soluble CD4 activates Env for coreceptor-dependent fusion and reveals blocking activities of antibodies against cryptic conserved epitopes on gp120. J. Virol. **74:**326–333.

46. **Steger, H. K., and M. J. Root.** 2006. Kinetic dependence to HIV-1 entry inhibition. J. Biol. Chem. **281:**25813–25821.

47. **Stiegler, G., R. Kunert, M. Purtscher, S. Wolbank, R. Voglauer, F. Steindl, and H. Katinger.** 2001. A potent cross-clade neutralizing human monoclonal antibody against a novel epitope on gp41 of human immunodeficiency virus type 1. AIDS Res. Hum. Retroviruses **17:**1757–1765.

48. **Sullivan, N., Y. Sun, J. Li, W. Hofmann, and J. Sodroski.** 1995. Replicative function and neutralization sensitivity of envelope glycoproteins from primary and T-cell line-passaged human immunodeficiency virus type 1 isolates. J. Virol. **69:**4413–4422.

49. **Tan, K., J. Liu, S. Wang, S. Sgen, and M. Lu.** 1997. Atomic structure of a thermostable subdomain of gp41. Proc. Natl. Acad. Sci. USA **94:**12303–12308.

50. **Trkola, A., M. Purtscher, T. Muster, C. Ballaun, A. Buchacher, N. Sullivan, K. Srinivasan, J. Sodroski, J. P. Moore, and H. Katinger.** 1996. Human monoclonal antibody 2G12 defines a distinctive neutralization epitope on the gp120 glycoprotein of human immunodeficiency virus type 1. J. Virol. **70:**1100–1108.

51. **Weiss, C. D.** 2003. HIV-1 gp41: mediator of fusion and target for inhibition. AIDS Rev. **5:**214–221.

52. **Weissenhorn, W., A. Dessen, S. C. Harrison, J. J. Skehel, and D. C. Wiley.** 1997. Atomic structure of the ectodomain from HIV-1 gp41. Nature **387:**426–430.

53. **Wild, C., T. D. C. Shugars, T. K. Greenwell, C. B. McDanal, and T. J. Matthews.** 1994. Peptides corresponding to a predictive α-helical domain of human immunodeficiency virus type 1 gp41 are potent inhibitors of virus infection. 1994. Proc. Natl. Acad. Sci. USA **91:**9770–9774.

54. **Williamson, C., L. Morris, M. F. Maughna, L. H. Ping, S. A. Dryga, R. Thomas, E. A. Reap, T. Cilliers, J. van Harmelen, A. Pascual, G. Ramjee, G. Fray, R. Johnston, S. A. Karim, and R. Swanstrom.** 2003. Characterization and selection of HIV-1 subtype C isolates for use in vaccine development. AIDS Res. Hum. Retroviruses **19:**133–144.

55. **Zwick, M. B., A. F. Labrijn, M. Wang, C. Spenlehauer, E. O. Saphire, J. M. Binley, J. P. Moore, G. Stiegler, H. Katinger, D. R. Burton, and P. W. Parren.** 2001. Broadly neutralizing antibodies targeted to the membrane-proximal external region of human immunodeficiency virus type 1 glycoprotein gp41. J. Virol. **75:**10892–10905.